# The effect of band structure on sputtering

Ming Tan and B.V. King

Physics Department, University of Newcastle, NSW 2308, Australia

## Abstract

Using one-color two step ionisation schemes, we have measured using resonant ionisation spectroscopy (RIS) the number of Ni atoms ejected in the ground state ($a^3F_4$) and an electronically excited state ($a^3D_3$) state from both $Ni_3Al$ and pure Ni surfaces. The ratio of the RIS signal from the $a^3D_3$ state to that from the $a^3F_4$ state is $1.07\pm0.03$ for $Ni_3Al$ and $1.05\pm0.08$ for pure Ni. To within experimental error, we saw no difference between pure Ni and the alloy in the relative sputter yield of Ni atoms in the excited $a^3D_3$ state compared to ground $a^3F_4$ state. There is a difference in the electronic band structure between pure Ni and $Ni_3Al$. The above result indicates the different band structure does not influence the relative sputter yields of excited states.

## Introduction

When bombarded by energetic ions, metal surfaces emit various particles including secondary ions, clusters and ground and excited state atoms. During sputtering, classical momentum transfer between the incident ion and target atoms takes place. In addition target atoms may be electronically excited or ionised. The momentum transfer leads to sputtering of particles. Electronic events occurring near the surface can determine the formation of secondary ions or excited secondary neutrals. An understanding of the basic mechanisms related to these electronic events is of fundamental and practical interest.

It is however difficult to analyse ejected secondary neutrals, either in the ground or excited states, because a mass spectrometer cannot directly detect them. In order to analyse secondary neutrals, the ejected neutrals must be ionised, typically by an electron beam, electron gas or laser. Of these techniques, laser postionisation is the most sensitive. It also allows state-selective ionisation so that both ground state and electronically excited neutrals may be separately measured. Results from laser postionisation measurements [1] on Ni show that the magnitude of the excitation energy, the electronic configuration and the character of the band structure play an important role in the formation of the excited atoms. For example in pure Ni, there are more atoms sputtered into the excited states $a^3D_3$ and $a^3D_2$ than the ground state $a^3F_4$. This observation has been explained by the resonant electron transfer model [2-4]. The aim of this study is to examine the resonant electron transfer model by measuring the ratio of atoms sputtered in the $a^3D_3$ state to those in the $a^3F_4$ state from pure Ni and from $Ni_3Al$, using RIS.
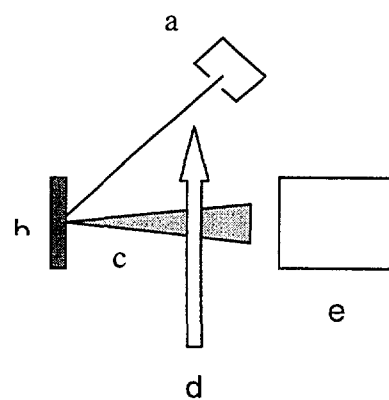


Figure 1. Schematic diagram of a laser postionisation mass spectroscopy: (a) primary ion source, (b) target, (c) ejected particles, (d) laser pulse beam, (e) mass spectrometer

## Experimental procedure

Figure 1 schematically shows the basic setup of a laser postionisation mass spectroscopy. Argon ions are produced in the ion source and electrostatically accelerated to 4keV and then focused at 45° incidence onto a 3mm spot on the target. A laser pulse of 8 ns with a cross section of 1mm x 8mm was positioned 12mm above the target surface. Neutral atoms sputtered in a specific quantum state are selectively ionised by tuning the laser wavelength and extracted into a time-of-flight mass spectrometer and subsequently counted by a microchannel plate detector. One-color two step schemes were
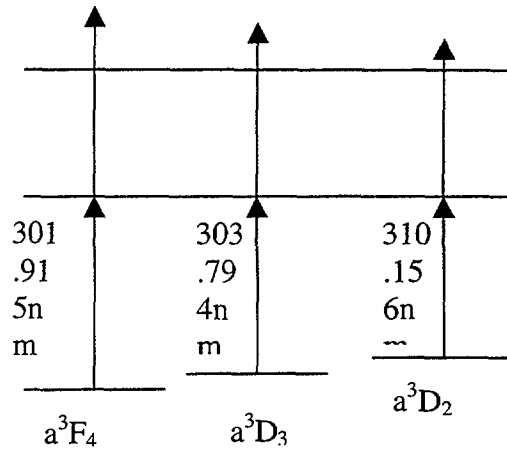


Figure2. One-color two step ionisation schemes used in this study

employed to ionise sputtered atom, as shown in Figure 2. The $a^3F_4$ is the ground state of Ni atoms and the $a^3D_3$ and $a^3D_2$ are excited states. The $a^3F_3{}^0$ is the resonant intermediate state and IP stands for the ionisation potential. For such ionisation schemes, two photons are required to ionise one atom. One photon excites an atom to the resonant intermediate state and subsequently this excited atom absorbs a second photon from the same laser field and become ionised. The ionisation efficiency depends mainly on the ionisation cross section.

Figure 3 shows a timing scheme for detecting RIS signal. The flight time of primary ions from the ion source to the target is 10μs. $\tau_D$ is the delay time between the primary ion pulse and the laser pulse. $\Delta\tau_I$ is the width of ion pulse. $\tau_E$ is a flight time of sputtered atoms from the target to the laser beam and $\tau_m$ is a flight time of laser-ionised atom in the extraction field. Sputtered atoms have a distribution of velocity. Faster sputtered atoms have a smaller $\tau_E$ and after being ionised, they take less time to reach MCP owing to their higher initial velocities at which they enter the extraction field and $\tau_m$ is correspondingly shorter. The $\tau_m$ of photoions of different initial velocities was measured by changing the delay time ($\tau_D$) between the primary ion pulse and the laser pulse. When $\Delta\tau_I$ is 200ns and $\tau_D$ is chosen to be 11μs, atoms whose $\tau_E$ is 0.8-1.0μs are ionised and a RIS peak appears at $\tau_m = 4.8$μs. When $\tau_D$ is 18μs, $\tau_E$ values of measured atoms range from 7.8-8.0μs and a RIS peak was observed at $\tau_m = 6.6$μs. In the RIS intensity measurements, the MCP is switched on 4.8μs and off 6.8μs after laser fires. This MCP gate can detect photoionised atoms whose $\tau_E$ ranges from 0.9 to 8.0μs. The kinetic energy is roughly estimated to be 54eV and 0.68eV for atoms sputtered with an $\tau_E$ of 0.9μs and 8μs, respectively. The RIS measurements were performed by changing the delay time ($\tau_D$) between the primary ion pulse and the laser pulse. From the RIS versus $\tau_D$ measurements, the relative intensity of atoms ejected in a specific atomic state can be determined.
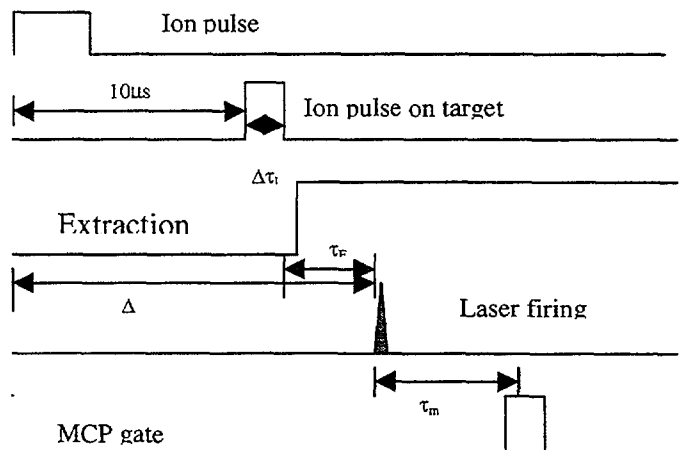


Figure 3. Timing scheme for RIS

The base pressure of the UHV chamber in which the target and MCP detector are assembled is $1.4 \times 10^{-9}$mbar and the operating pressure is $2.1 \times 10^{-8}$mbar. The time required that a clean metal surface adsorbs a monolayer of contamination under this base pressure is theoretically estimated to be 15 min. In order to reduce contamination, the measurements were done with a 2μs pulse. The measurement time is shorter than 3 min.

We examine the cleanliness of a target surface by measuring the RIS intensity. The RIS intensity increases as the surface contamination decreases. The ion beam was continuously rastered across a surface area of 5.7mm x 5.7mm, and subsequently the RIS intensity was measured. The cleaning and RIS measurement was repeated until the RIS intensity was found to stay unchanged. Then the target was believed to be clean and measurements were performed.

## Results

Figure 4 shows $\tau_D$ distributions of the RIS of Ni atoms ejected in $a^3F_4$ and $a^3D_3$ states from $Ni_3Al$. Most of Ni atoms sputtered in $a^3F_4$ and $a^3D_3$ states were observed at $\tau_D$ of 11.5 – 17.5μs, which is identical to $\tau_E$ of 1-7μs.

We have measured the RIS intensity of atoms sputtered in $a^3F_4$ and $a^3D_3$ states from pure Ni and $Ni_3Al$ single crystals, with $\tau_E$ ranging from 1 to 7μs (kinetic energies being 0.9 - 44eV. Four independent measurements were performed for all the RIS intensities. The laser power for these measurements is 1.0 – 1.2mJ/pulse. Table 1 gives normalised RIS intensities and shows that the $a^3F_4$ RIS intensity is almost equal to the $a^3D_3$ intensity for $Ni_3Al$ and pure Ni. The RIS ratio of $a^3D_3$ to $a^3F_4$ is 1.046 for pure Ni, and 1.074 for $Ni_3Al$.
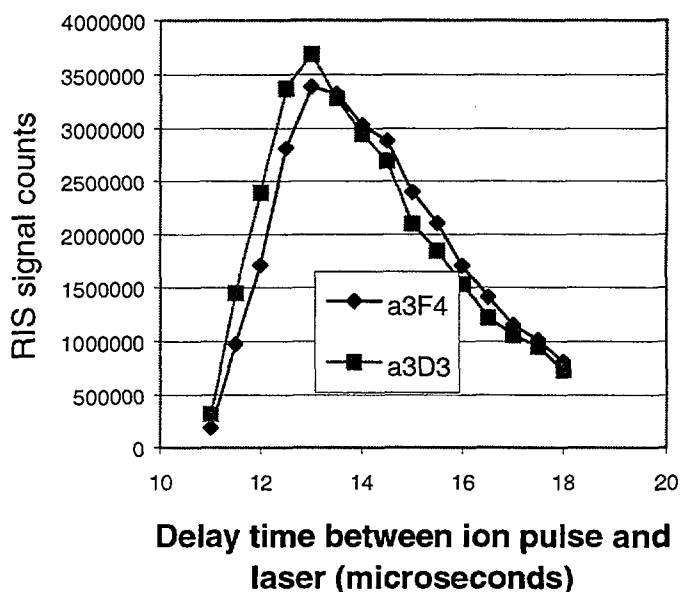


**Delay time between ion pulse and laser (microseconds)**

Figure 4 RIS intensity versus delay time for ground and excited states in $Ni_3Al$

## 4. Discussion

The resonant electron model assumes that the formation of a sputtered atom can be regarded as a departing ion picking up an electron from the valence band and that the orbital energy and shape of the valence electron is preferentially preserved. Consequently, the population of atoms sputtered in a specified quantum state can depend not only on the excitation energy but also on the coupling between the valence electron and the final state of the atom. The electronic configuration of Ni atoms ejected in the $a^3D_3$ and $a^3D_2$ states $(3d^94s^1)$ is closer to the valence electron of Ni $(3d^{9.4}4s^{0.6})$ than that of the ground state $(3d^84s^2)$. Due to the weaker coupling of the ground state to the valence electron, the ground state $a^3F_4$ is less populated than the $a^3D_3$ and $a^3D_2$ states.

Table 1 RIS signal of Ni atoms ejected in $a^3F_4$ and $a^3D_3$ states from $Ni_3Al$ and Ni

| Ni₃Al | | Pure Ni | |
|---|---|---|---|
| $a^3F_4$ | $a^3D_3$ | $A^3F_4$ | $a^3D_3$ |
| 43.2 | 48.1 | 35.1 | 41 |
| 44.2 | 47.7 | 37.6 | 37.8 |
| 43.8 | 46.8 | 39.2 | 39.5 |
| 47.4 | 48.9 | 36.8 | 37.2 |
| Average 44.6 | Average 47.9 | Average 37.2 | Average 38.9 |

The valence electron configuration of $Ni_3Al$ is calculated to be $3d^{8.4}4s^{1.6}$ [5]. The difference in electronic structure between the $Ni_3Al$ band $(3d^{8.74}4s^{1.26})$ and the atomic ground state $a^3F_4$ $(3d^84s^2)$ is much smaller than that between the Ni band $(3d^{9.4}s^{0.6})$ and the $a^3F_4$ state. According to the resonant tunneling model, the probability of a valence electron resonantly transferring into the $a^3F_4$ state $(3d^84s^2)$ in the $Ni_3Al$ single crystal should be larger than in the Ni single crystal due to the stronger coupling of an atomic ground state with the valence band of the alloy. Therefore, if the model holds true, the population ratio of $a^3D_3$ to $a^3F_4$ in the $Ni_3Al$ crystal should be smaller than in the Ni crystal.

The RIS intensity is given by I = nVP where n is the population density that indicates the number per unit volume at the laser beam region of atoms ejected in a specific quantum state, V is the sampling volume and P is the ionisation probability of one atom. Since the experimental conditions for the $Ni_3Al$ alloy are the same as those for the Ni metal, the V and P ratios of $a^3D_3$ to $a^3F_4$ for the alloy are identical to those of the metal. Therefore, the population ratio change is reflected in the RIS signal intensity ratio. However, the expected decrease in the RIS ratio was not observed in $Ni_3Al$. Much research is required to confirm the resonant electron transfer model.

## 5. Summary

The RIS ratio of $a^3D_3$ to $a^3F_4$ in $Ni_3Al$ is almost identical to that in pure Ni. We did not observe the band structure effect on sputtering of Ni atoms in $a^3F_4$ and $a^3D_3$ states from $Ni_3Al$ and pure Ni. The band structure effect of sputtering is awaiting further examinations.

## 6. References

[1]   B.J. Garrison, N. Winograd, R. Chatterjee, Z. Postawa, A. Wucher, E. Vandeweert, P. Lievens, V. Philipsen, R. Silverans, Rapid Commun. Mass Spectrom. 12, 1266(1998).

[2]   C. He, Z. Postawa, S. Rosencrance, R. Chatterjee, B.J. Garrison, and N. Winograd, Phys. Rev. Lett 75, 3950(1995).

[3]   E. Vandeweert, V. Philipsen, W. Bouwen, P. Thoen, H Weidele, R. Silverans, and P. Lievens, Phys. Rev. Lett. 78, 138(1997).

[4]   E. Veje, Phys. Rev. B28, 5029(1983).

[5]   Zs. Kovcs, et al, Phys. Rev. B54, 8501(1996).